Schweizerische Eidgenossenschaft
Confédération suisse
Confederazione Svizzera
Confederaziun svizra

Department of the Environment,
Transport, Energy and Communication DETEC

Swiss Federal Office of Energy SFOE
Energy Research

Final report

Efficient Hydrogen Fueling

Research in the field of gaseous hydrogen fast filling for passenger cars

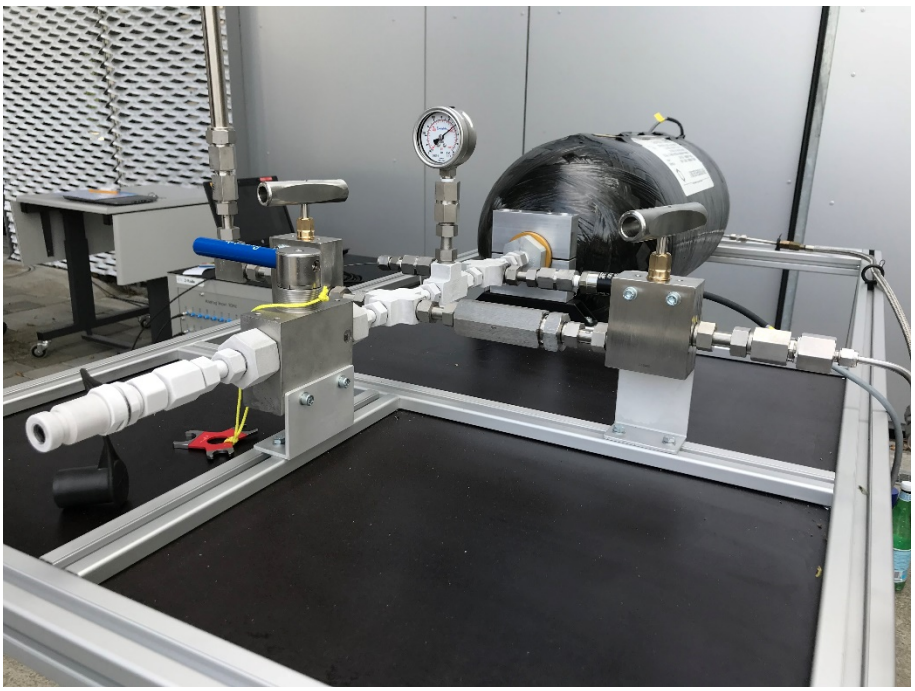

Empa
Materials Science and Technology

Date: 16 December 2019

Place: Bern

Publisher:
Swiss Federal Office of Energy SFOE
Research and development
CH-3003 Bern
www.bfe.admin.ch
energieforschung@bfe.admin.ch

Agent:
Empa
Überlandstrasse 129, CH-8600 Dübendorf
https://www.empa.ch/web/empa

Author:
Patrick Stadelmann, Empa, patrick.stadelmann@empa.ch

SFOE head of domain: Stefan Oberholzer, stefan.oberholzer@bfe.admin.ch
SFOE programme manager: Stefan Oberholzer, stefan.oberholzer@bfe.admin.ch
SFOE contract number: SI/501579-01

Summary

Within the framework of the efficient hydrogen fueling (eHF) project, the energy demand of the pre-cooling system at Empa's hydrogen filling station was analyzed. The assessment showed that under the current conditions a significant amount of energy is required. Moreover, the temperature rise within vehicle tanks during fast refueling of hydrogen was investigated by means of measurements and CFD simulations. For the experimental filling tests, a mobile test bench was developed that allows spatial measurements of the temperature evolution in a tank during refueling. The test setup was mounted on a frame enabling easy transport to the hydrogen refueling station (HRS). Several filling tests were carried out for experimental observations and validation of the computational model. A set of relevant parameters for the refueling process was identified with which a test matrix was created. Besides changing seasonal conditions, the influence of the injection nozzle diameter, initial tank pressure and fueling protocol was investigated. Among other things, temperature differences of up to 20°C were observed during refueling at inlet gas velocities of less than 5 m/s. Higher inlet gas velocities led to a homogeneous temperature distribution. In addition, the developed computational model was tested against experimental data to accurately predict the temperature development in a tank. Depending on model parameter settings, the calculated temperature profile was found in good agreement with experimental data and errors on the calculated maximum gas temperatures were below 6%.

Zusammenfassung

Im Rahmen des eHF Projekts wurde der Energiebedarf des Vorkühlsystems an der Wasserstofftankstelle der Empa analysiert. Man konnte aufzeigen, dass unter den aktuellen Bedingungen einen erheblichen Energiebedarf besteht. Ausserdem wurde der Temperaturanstieg in Fahrzeugtanks während schnellen Wasserstoffbetankungen mittels Messungen und CFD-Simulationen untersucht. Für die experimentellen Füllversuche wurde ein mobiler Prüfstand entwickelt, mit dem die Temperaturentwicklung in einem Tank beim Betanken räumlich gemessen werden kann. Es wurden mehrere Füllversuche zur experimentellen Beobachtung und Validierung des Berechnungsmodells durchgeführt. Dabei wurde neben wechselnden saisonalen Bedingungen auch der Einfluss von Einspritzdüsendurchmesser, Anfangsdruck des Tanks und Betankungsprotokoll untersucht. Bei Einlassgeschwindigkeiten von weniger als 5 m/s konnten Temperaturunterschiede von bis zu 20°C beobachtet werden. Höhere Einlassgeschwindigkeiten führten zu einer homogenen Temperaturverteilung. Zudem wurde das entwickelte Berechnungsmodell anhand der experimentellen getestet, um die Temperaturentwicklung in einem Tank genau vorhersagen zu können. Abhängig von den verwendeten Modellparametern stimmte das berechnete Temperaturprofil mit den Versuchsdaten gut überein und der Fehler lag unter 6%.

Résumée

Dans le contexte du project eHF, la demande en énergie du système de refroidissement de la station de remplissage d'hydrogène de l'Empa a été analysée. L'évaluation a montré que, dans les conditions actuelles, une quantité importante d'énergie est nécessaire. En plus, l'augmentation de la température à l'intérieur de réservoirs des véhicules pendant le ravitaillement rapide en hydrogène a été étudiée au moyen de mesures et de simulation CFD. Pour les essais expérimentaux de remplissage, un banc d'essai mobile a été développé qui permet de mesurer l'évolution spatiale de la température à l'intérieur d'un réservoir pendant le remplissage. Le montage d'essai a été installé sur un châssis permettant un transport aisé jusqu'à la station de ravitaillement en hydrogène. Plusieurs essais de remplissage ont été réalisés pour des observations expérimentales et la validation du modèle de calcul. Un ensemble de paramètres pertinents pour le processus de ravitaillement en hydrogène a été identifié et une matrice d'essai a été créée à partir de ces paramètres. En plus de changer les conditions saisonnières, l'influence du diamètre de la buse d'injection, de la pression initiale du réservoir et du protocole de ravitaillement a été étudiée. Entre autres, des différences de température allant jusqu'à 20°C ont été observées lors du

ravitaillement en carburant à des vitesses de gaz à l'entrée inférieures à 5 m/s. Des vitesses de gaz d'entrée plus élevées ont permis d'obtenir une distribution homogène de la température. De plus, le modèle de calcul mis au point a été testé par rapport à des données expérimentales pour prédire avec précision l'évolution de la température dans un réservoir. Selon les réglages des paramètres du modèle, le profil de température calculé a été trouvé en bon accord avec les données expérimentales et les erreurs sur les températures maximales calculées du gaz étaient inférieures à 6 %.

Contents

List of abbreviations

APRR	Average Pressure Ramp Rate
B2B	Back to Back
CEP	Clean Energy Partnership
CFD	Computational Fluid Dynamics
CHT	Conjugate Heat Transfer
DE	Daily Energy use
DDH	Daily Delivered Hydrogen
EHF	efficient Hydrogen Fueling
EI	Energy Intensity
HRS	Hydrogen Refueling Station
HX	Heat Exchanger
NIST	National Institute of Standards and Technology
NWP	Nominal Working Pressure
PCU	Pre Cooling Unit
P&ID	Piping and Instrumentation Diagram
SAE	Society of Automotive Engineers
SOC	State of Charge
SST	Shear Stress Transport
WP	Work Package

1 Introduction

The eHF project aims to investigate hydrogen fast filling processes by means of measurements and CFD simulations. In order to have a solid scientific background, the project consists of an experimental work package (WP1) and a simulation work package (WP2). Several filling tests were carried out to validate the calculation model and to be able to carry out experimental observations.

For the experimental filling tests, a mobile test bench was developed that allowed spatial measurements of temperature development in a tank during refueling. A set of relevant parameters for the refueling process was identified with which a test matrix was created. In total 22 experiments were performed, including 15 tank fillings and 7 tank defuelings.

A computational model was developed and tested against experimental data to accurately predict the temperature development in a tank. The computational model provides a detailed spatial resolution of the vehicle tank, which is required for a detailed analysis of the hydrogen fast filling processes.

2 Context

2.1 Background / State of the art

Generally, a hydrogen refueling station (HRS) consists of a hydrogen source, a compressor, a storage system , a cooling system and one or more fueling points. Figure 1 shows a simplified schematic of a HRS setup.

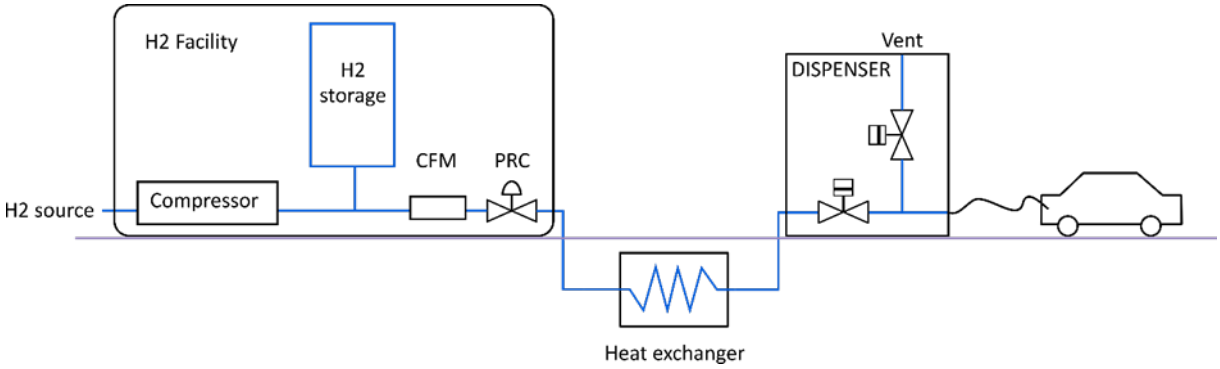

Figure 1 Generalized setup of a 70 MPa HRS, consisting of a hydrogen supply, a compressor, a storage system, a cooling system and a dispenser.

The nominal working pressure (NWP) for hydrogen-powered passenger cars is 70 MPa. To be able to deliver this pressure, a 90 MPa high-pressure storage system with sufficient capacity to meet customer demand is required. Accordingly, a compressor is needed to refill the dispensed hydrogen. Commonly, a piston or ionic compressor is used, which are selected according to the design of the station, considering station capacity, energy consumption, cost-effectiveness, etc.

The requirement for a short refueling time (3-5 min) for hydrogen vehicles is a challenge, as the rapid compression of the gas leads to high temperatures in the tank, which can compromise the mechanical integrity of the system. With modern carbon reinforced type IV tanks the maximum allowable temperature is set to 85°C. In addition to safety considerations, the rise in temperature has a negative effect on the gas density and thus on the total amount of gas injected into the tank during filling. In order to avoid high temperatures, the current technical approach for hydrogen refueling of passenger cars is to pre-cool the gas before injecting it into the tank. The refueling procedure complies with the internationally recognized refueling protocol SAE J2601 [1], which ensures that the temperature limit is not exceeded. For a 70 MPa fast refueling of a passenger car the hydrogen is pre-cooled to -40°C (category H70-T40). Higher precooling temperatures are possible, but inherently lead to a prolonged refueling. Figure 2 gives an overview of the refueling included in the SAE (ver. 2016). This pre-cooling leads to an increased energy consumption and adds complexity to the system.

Standard Designation		**H35**		**H70**	
Storage Capacity Classification		Small Capacity (e.g. Motorcycle) (< 1.2 kg)	**Light Duty (1.2 - 6.0 kg)**	Small Capacity (e.g. Motorcycle) (< 2.0 kg)	**Light Duty (2.0 - 10.0 kg)**
SAE J2601 Fueling Protocols	**T40**	Not Included	Included	Not Included	Included
	T30				
	T20				
Station Dispenser Type Category	**T10**				
	T_Ambient				

Figure 2 Refueling included in the SAE J2601 (ver. 2016) [1]

2.2 Motivation of the project

As discussed in the previous section, the cooling system at a hydrogen filling station requires energy. In this section an in-depth analysis of the pre-cooling unit installed at the HRS at Empa is presented.

The pre-cooling unit (PCU) at Empa uses a compression chiller and an aluminum heat exchanger (HX) with a large thermal mass to generate the required low fuel delivery temperature. The buffering effect of the large thermal mass allows to fill three vehicles back to back (B2B). Note that there are different types of HX that can be used, each has its own advantages and disadvantages. A detailed comparison between large and small HX options can be found in [2].

In general, the cooling requirement of the PCU consists of two parts: the cooling required to pre-cool the dispensed hydrogen and the overhead cooling required to keep the HX at a constant low temperature. In order to decouple the cooling energy associated with refueling and the overhead energy consumption of the PCU, a two-stage approach was used [2]. First, the energy to maintain the HX cold throughout the day is determined when the dispenser is idle. This provides the daily electric energy consumption for overhead cooling ($DE_{overhead}$). Figure 3 shows the correlation between daily overhead energy consumption and ambient temperature from an analysis over several months.

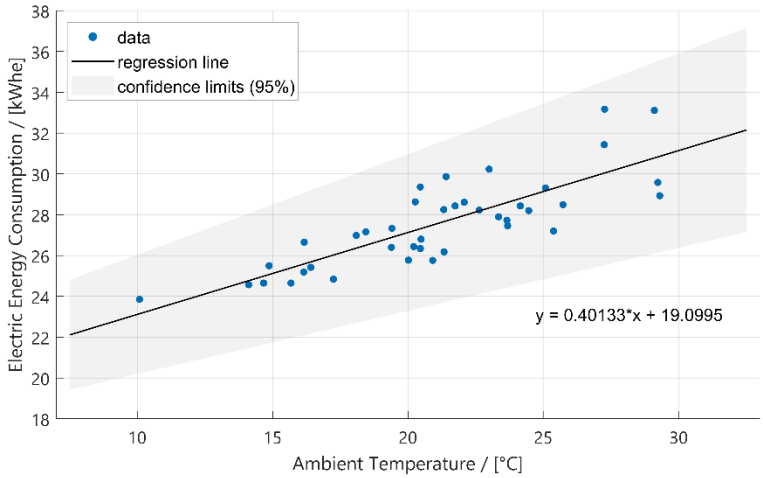

Figure 3 Evaluation of the overhead electric energy consumption of the PCU at Empa depending on the average ambient temperature

The assessment of the daily overhead consumption of the PCU shows that the electricity consumption strongly depends on the ambient conditions. As expected, the energy required to keep the heat exchanger cold increases with higher ambient temperatures. In addition to a few outliers, the determined electrical energy demand for refueling also shows a clear trend.

Second, the daily energy consumption on days when refueling occurred was also determined (DE_{total}). Subtracting these two energy consumptions and taking the ambient temperature into account yields the energy consumption needed to refuel hydrogen. Dividing this energy consumption by the daily delivered hydrogen mass (DDH_2) results in the electrical energy input needed of the PCU per kilogram of dispensed hydrogen (EI_{PCU}):

$$EI_{PCU} = \frac{DE_{total} - DE_{overhead}}{DDH_2}$$

The analysis of the PCU at Empa showed, that on a warm summer day the electric energy required for the daily overhead cooling of the HX is in the order of 30 kWh_e. Whereas the electric energy needed for cooling the dispensed hydrogen is approximately 0.5 kWh_e/kg. Note that the energy intensity of a HRS highly depends on the utilization level of the station. As the HRS utilization level increases, the overall electricity consumption for cooling gets smaller, as shown in Figure 4.

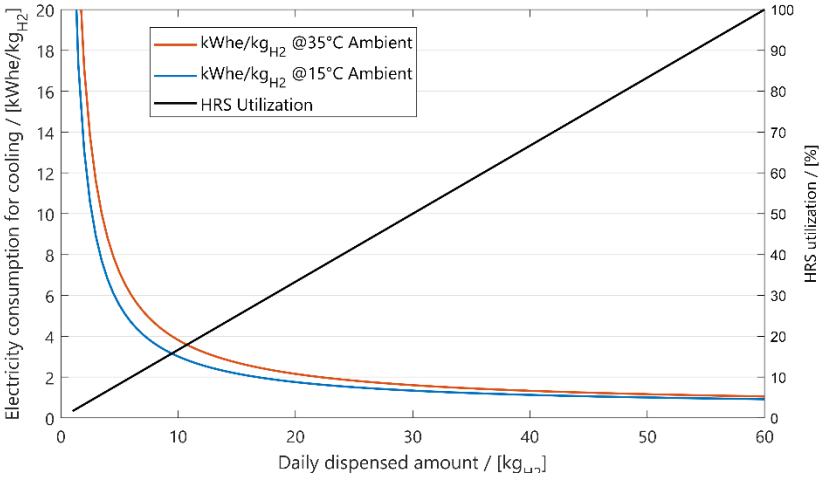

Figure 4 Electrical energy consumption of the PCU at Empa depending on the utilization of the HRS

This energy consumption is significant and determines the cost of such a pre-cooling unit. Optimizing the pre-cooling at a HRS will increase the well-to-tank efficiency as well as reduce capital and operational cost of the filling station.

2.3 Goals

According to the SAE J2601 fueling protocol, hydrogen needs to be pre-cooled most commonly to -40°C to ensure tank integrity and full fillings within minutes. This pre-cooling adds complexity, energy demand and capital as well as operational costs. The aim of this project is to conduct measurements of hydrogen fast fillings, capturing the spatial gas temperature evolution as well as the tank wall temperature. These measurements allow the validation of a 3-dimensional CFD model.

Goals:

- Conduct measurements to investigate the effects of various parameters on the refueling process
- Create a validated CFD model to accurately predict the temperature development within a tank on the basis of the measurements

3 Approach and methodology

In this Chapter, the developed experimental setup and computational model are presented. Section 3.1 briefly describes the built test bench for measuring the temperature development inside hydrogen tanks during refueling as well as the filling tests performed, while section 3.2 explains the modelling approach of the simulation model.

3.1 Experimental filling tests (WP1)

3.1.1 Experimental setup

For these experiments, a 36 liters tank is equipped with pressure and temperature sensors. In order to be able to measure the temperature inside the tank, we have designed and constructed a thermocouple tree. Figure 5 shows the thermocouple tree (left) and one of the used injection nozzles with a length of 100 mm and an injection diameter of 6 mm (right).

Figure 5 (Left) in-house developed thermocouple tree, (right) injection nozzle

In our experiments, we have tested injectors with a diameter of 3 and 6 mm. Alternatively, we have also designed a nozzle geometry that is angled 30° from the axial center line of the cylinder. However, in this study we focus only on straight nozzle geometries.

The thermocouple tree consists in total of 8 thermocouples, which are sealed by a stuffing box. The transmitter cables are guided to the outside. In addition six thermocouples were placed on the tank surface (three on the bottom and three on the top) using a reinforced aluminum tape. These external wall thermocouples have a weld pad that enables good thermal contact with the tank wall. The detailed position of the tank thermocouples is shown in Figure 6. All temperature measurements are placed in the vertical center plane. Note that the probes in the gas region are located in the rear end of the tank to avoid excessive disturbance of the incoming gas. However, this cannot be completely avoided with an intrusive measurement technique.

In addition, another thermocouple was placed at the intake. In total 15 type K thermocouples with special error limits (±1.1°C or 0.4%) were installed. Whereas the pressure sensors used to measure the tank and inlet pressure have a relative accuracy of 0.3%.

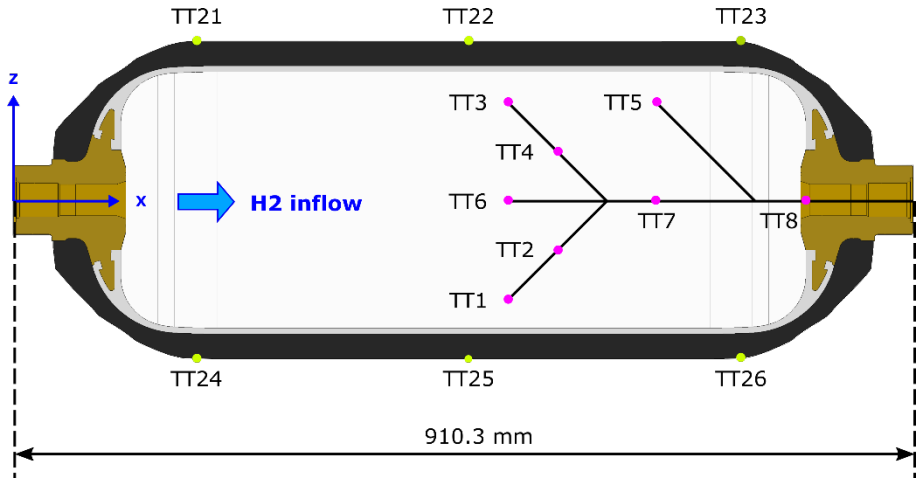

Figure 6 Position of internal thermocouples (TT1 - TT8) and thermocouples placed on tank wall (TT21 – TT26)

The test setup is mounted on a mobile frame on rollers, which can easily be transported to the HRS for the measurements, as shown in Figure 7. For monitoring and logging purposes the pressure and temperature sensors are automatically read using LabVIEW. A detailed piping and instrumentation diagram (P&ID) of the realized test bench is presented in Appendix 1.

3.1.2 Description of the experiments

The test bench was positioned at Empa next to the HRS as can be seen in Figure 7, which shows two general views of the setup on the first day of measurements. One can see the completely installed experimental setup as well as the electronic cabinet for data acquisition. Signs and a safety cordon visually secure the area.

Figure 7 General views of the setup on the first day of measurements

Several measurements were taken in the summer and winter months. In this report, we present only the most relevant filling tests with a focus on homogeneous temperature conditions needed for a simple model validation. One exception is fill n°2, which has a reduced flow rate compared to the others. A summary of the performed fueling tests is shown in Table 1. Each parameter is changed at least once to assess it's impact on the fueling

compared to the reference case. Besides different seasonal conditions, the influence of the injection nozzle diameter, initial tank pressure and fueling protocol was investigated. It is expected that the higher velocities using an alternative nozzle with a smaller diameter result in a more homogeneous temperature distribution within the vehicle tank. Whereas the variation of the initial tank pressure and the fueling protocol has a direct effect on the final temperature reached.

Table 1 Parameters of the investigated cases

Scenario	Fill	Injector diameter	Initial pressure	Fueling protocol	Season
Reference case	1	6 mm	100 bar	SAE A-70	Winter
Fueling protocol change	2	6 mm	100 bar	CEP A-70	Summer
Fueling protocol and injection diameter change	3	3 mm	100 bar	CEP A-70	Summer
Fueling protocol, injection diameter and pressure change	4	3 mm	50 bar	CEP A-70	Summer
Fueling protocol, injection diameter and pressure change	5	3 mm	300 bar	CEP A-70	Summer

Figure 8 shows a standard look-up table of the SAE J2601 (ver. 2010) fueling protocol for non-communication 70 MPa fueling at -40°C. It should be noted that the Average Pressure Ramp Rate (APRR) is dependent on the ambient temperature as well as fuel delivery temperature category and vehicle tank capacity.

In the example below it can be seen that linear interpolation is used to derive the actual parameters from the table values. A one-dimensional interpolation for the APRR (based on the ambient temperature, see position 1) and a two-dimensional interpolation for the target pressure. If one of the interpolation values is in the "no refueling" zone of the table, the dispenser does not refuel the vehicle.

A-70 1-7kg		Average Pressure Ramp Rate, APRR (MPa/min)	Fueling Target Pressure, P_{target} (MPa)										
			Initial Tank Pressure, P_0 (MPa)										
			2	5	10	15	20	30	40	50	60	70	> 70
Ambient Temperature, T_{amb} (°C)	> 50	no fueling	no fueling	no fueling	no fueling	no fueling	no fueling	no fueling	no fueling	no fueling	no fueling	no fueling	no fueling
	50	11.4	73.5	73.2	73.0	72.8	72.6	72.4	72.2	72.0	71.9	72.2	no fueling
	45	15.7	73.9	73.6	73.3	73.0	72.8	72.5	72.3	72.0	71.8	72.1	no fueling
	40	19.8	74.2	73.9	73.6	73.2	73.0	72.6	72.2	72.0	71.8	72.0	no fueling
	35	23.7	74.5	74.1	73.6	73.3	73.1	72.7	72.3	72.0	71.8	72.0	no fueling
1	30	27.4	74.1	73.8	73.2	72.7	72.5	71.9	71.4	71.0	70.6	71.0	no fueling
	25	28.2	73.6	73.3	72.6	72.3	71.7	70.9	70.4	69.9	69.3	no fueling	no fueling
	20	28.2	73.2	72.8	72.0	71.4	2	70	69.3	3	68.2	no fueling	no fueling
	10	28.2	72.0	71.5	70.6	70.0		68.2	67.2		65.8	no fueling	no fueling
	0	28.2	70.9	70.3	69.3	68.5	67.9	66.4	65.2	64.0	63.5	no fueling	no fueling
	-10	28.2	69.8	69.2	67.9	67.1	66.1	64.4	63.0	61.6	no fueling	no fueling	no fueling
	-20	28.2	68.9	67.9	66.6	65.5	64.3	62.4	60.7	59.1	no fueling	no fueling	no fueling
	-30	28.2	67.8	66.7	65.2	63.7	62.5	60.4	58.3	56.4	no fueling	no fueling	no fueling
	-40	28.2	67.3	66.5	65.0	63.7	62.5	60.1	58.3	56.4	no fueling	no fueling	no fueling
	< -40	no fueling	no fueling	no fueling	no fueling	no fueling	no fueling	no fueling	no fueling	no fueling	no fueling	no fueling	no fueling

Figure 8 SAE-J2601 Non-Communication fueling table – Type A-70 fueling ramp rates and pressure targets for tank capacities 1-7 kg

The CEP look-up tables use the same logic, but differ in the APRR, which is generally slower at warm ambient temperature conditions. In addition, the target pressure is lower.

3.2 Computational model (WP2)

3.2.1 Model setup

The computational model is based on the open source CFD code OpenFOAM [3] and was developed according to information obtained from our own experiments and literature [4]. The mesh of the studied type IV tank was generated as a 3D model without simplifications using the snappyHexMesh utility supplied with OpenFOAM. SnappyHexMesh is a meshing tool that can generate meshes with hexahedra (hex) cells. As shown in Figure 9, the computational domain consists of four different sub-domains.

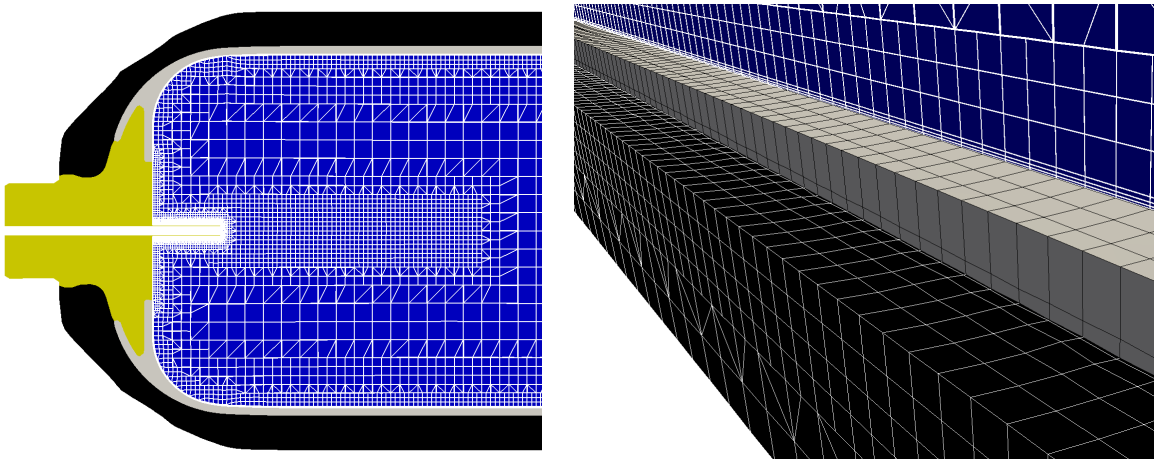

Figure 9 Computational domain geometry and grid details of the standard mesh

1. Gas region, describes the interior of the tank filled with hydrogen (blue)
2. Solid region 1, describes the internal plastic liner (gray)
3. Solid region 2, describes the external composite carbon fiber shell (black)
4. Solid region 3, describes the two aluminum alloy bosses at the tank ends (gold)

Generally, the computational model consists of a long cylindrical section with elliptical heads. The total number of elements over all sub-domains is 1'164'969 for the standard mesh. Dedicated mesh sensitivity studies have not been carried out at this stage. However, the computational grid was built according to best knowledge available. This is reflected in the different refinement levels depending on the sensitivity of the area e.g. fine resolution in the cells at the inlet or near the wall. The standard mesh uses a straight nozzle with an inner diameter of 6 mm, which extends 100 mm into the tank.

The heat transfer through the tank wall reduces the gas temperature significantly. To capture the heat transfer through the solid materials in conjunction with the changing temperature in the gas region, OpenFOAM's conjugated heat transfer (CHT) capability was used. Furthermore, the following available modelling options were chosen to capture the underlying physics as accurately as possible:

- The compressibility effects at high pressures were taken into account using a real gas equation of state to determine hydrogen properties (Peng-Robinson [5]);
- The k– w SST (Shear Stress Transport) turbulence model [6] was implemented to reproduce the occurring turbulent flow;

- The gravitational source term was included into the momentum equation to consider the buoyancy effects.

A detailed overview of the design parameters used in this study for the reference case is given in Table 2.

Table 2 Design parameter of the type IV tank [7]

Characteristics – type IV tank	Units	Value
General tank characteristics		
Internal gas volume	liters	36
External diameter	mm	320.8
Internal diameter	mm	258.8
Wall thickness liner (cylindrical section)	mm	6
Wall thickness carbon wrapping (cylindrical section)	mm	25
Internal liner surface area	m^2	0.61
Composite wrapping		
Density	kg/m^3	1600
Thermal conductivity	W/m/K	1.5
Specific heat capacity	J/kg/K	1400
Liner		
Density	kg/m^3	947
Thermal conductivity	W/m/K	0.36
Specific heat capacity	J/kg/K	1880
Aluminum boss		
Density	kg/m^3	2730
Thermal conductivity	W/m/K	167
Specific heat capacity	J/kg/K	900

Transient pressure and temperature profiles were imposed at the tank inlet boundary to reproduce the measured filling conditions, as shown in Figure 10 for the reference case. The flow at the inlet transient and is computed by the solver. A non-slip boundary condition was applied at inner tank and injection nozzle walls. At the outer tank and bosses walls, a constant heat transfer coefficient was imposed to determine the heat transfer to the environment, while the injection nozzle wall was considered adiabatic. Ambient temperature (11.5°C) was assumed to be constant throughout the filling. Initial conditions were defined by the measured temperature (11.5°C) and pressure in the tank (10 MPa), which were assumed to be uniform. The tank was conditioned before all of our experiments and therefore it was assumed that the tank walls, e.g. liner and composite, would initially be at the same temperature as the gas.

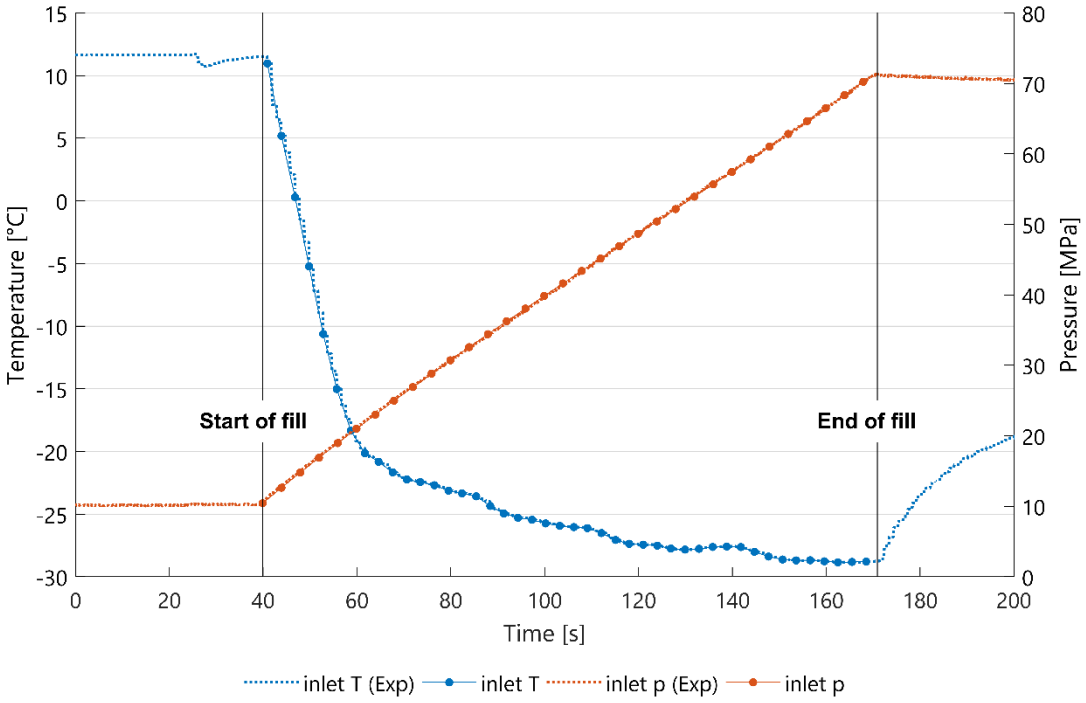

Figure 10 Applied temperature and pressure boundary condition at the tank inlet for the reference case simulation

3.2.2 Sensitivity study

In order to better assess the model capabilities, sensitivity analyses were carried out on boundary conditions and material properties. The settings of the reference case were used as a benchmark for the comparison. Depending on the variable analyzed, additional simulations were performed, where the investigated variable is varied from the nominal value. Table 3 gives an overview of the investigated parameters. A lower and upper limit was defined, which lies within the uncertainties.

Table 3 Variation of the investigated parameters

Parameter	Lower limit	Upper limit
Pressure	-1% Ref. case	+1% Ref. case
Temperature	-3°C Ref. case	+3°C Ref. case
Thermal conductivity of the plastic liner	-	2 x Ref. case

In addition, the Redlich-Kwong equation of state was implemented to check the influence on the temperature development and the influence on the total mass fueled. It is known from literature that the real gas behavior has to be modelled, but it should be noted that the available equations of state vary in their performance. Table 4 shows a density comparison of the Peng-Robinson and Redlich-Kwong [8] equation of state with NIST data [9] for hydrogen at different states (typical conditions for a hydrogen refueling).

Table 4 Density comparison of the Peng-Robinson and Redlich-Kwong cubic equation of state with NIST data

Thermodynamic state		Peng-Robinson		Redlich-Kwong	
T [°C]	p [MPa]	Density [kg/m^3]	Error [%]	Density, kg/m^3	Error, %
15°C	70 MPa	42.33	5.36	39.30	-2.17
15°C	10 MPa	8.12	2.49	7.91	-0.23
-30°C	70 MPa	47.79	5.95	43.98	-2.48
-30°C	10 MPa	9.63	3.12	9.30	0.37

It can be seen that the error in density for the Peng-Robinson equation of state is between 2.49% and 5.95%. While the Redlich-Kwong is able to model the density more accurately. At low pressures (10 MPa) the error lies below 0.5%, whereas at high pressures (70 MPa) the density is underestimated by 2.48%. Overall, it seems that Redlich-Kwong models the density more accurately than Peng-Robinson.

4 Results

In this Chapter, the experimental results and the developed simulation model are presented. Section 4.1 briefly summarizes the experiments, while in Section 4.2 the simulation results are compared to the measurements.

4.1 Experimental results

As mentioned, the measurements took place on different days and seasonal conditions. A summary of the tests performed with the most relevant parameters is given in Table 1, while the position of the tank thermocouples is shown in Figure 6.

Figure 11 shows the measured pressure and temperature evolution of the reference case using an injection nozzle with a diameter of 6 mm. For this experiment, the initial tank pressure was set to 10 MPa at an ambient temperature of 11.5°C. Based on these conditions, the APRR was set to 28.2 MPa/min in accordance to the SAE J2601 T40 fueling protocol (ver. 2010), see Figure 8. It can be seen that the temperature distribution in the gas region is not completely homogeneous, especially towards the end of the filling process. We measure temperature differences of up to 7°C between the individual thermal probes in the tank. In addition, the probes located in the upper rear part of the tank (e.g. TT03, TT04 and TT05) detect a temperature rise after completion of the filling, before decreasing again.

Furthermore, it can be seen that after filling, when the temperature already starts to decrease, the probes located in the lower part of the tank (e.g. TT01 and TT02) clearly measure a lower temperature by several degrees. This can be explained by buoyancy effects, which play a dominant role at lower gas velocities. Note that the forced gas circulation caused by the inflowing hydrogen, ceases after the completion of the refueling.

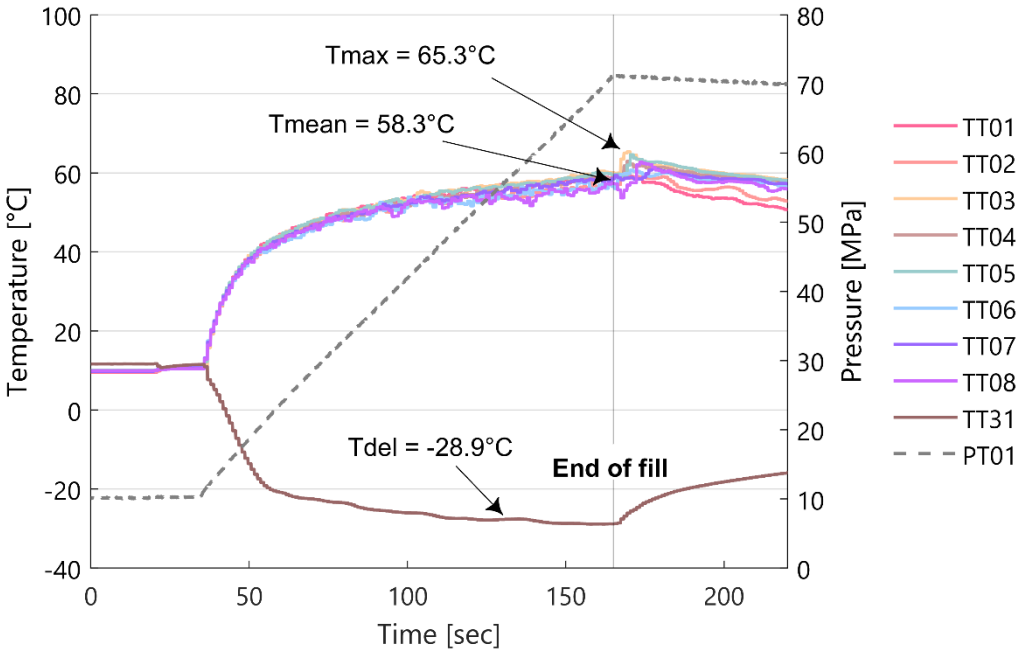

Figure 11 Reference case (6 mm injection Ø) – pressure and temperature measurements during filling on the test bench with an APRR of 28.2 MPa/min (according to SAE protocol). For this experiment, the initial tank pressure was set to 10 MPa at an ambient temperature condition of 11.5°C

The reference case seems to be a borderline case where the gas mixing due to the inflowing hydrogen is good enough to prevent a pronounced temperature stratification. However, it is expected that a further reduction of the inlet gas velocity would lead to a temperature stratification.

Figure 12 shows the measured pressure and temperature development of filling no. 2 using an injection nozzle with a diameter of 6 mm. For this experiment, the initial tank pressure was again set to 10 MPa at an ambient temperature of 27.8°C. Based on these initial conditions, the APRR was set to 16.8 MPa/min in accordance with the CEP A70 fueling protocol (ver. 2010). It can be seen that we achieved a similar precooling temperature as in the reference case, but due to the lower pressure ramp rate the gas mixing was worse in respect to the fueling shown in Figure 11. At some point around t=200 s the effect of temperature stratification becomes apparent. Note that a maximum temperature of 82°C was reached and a temperature difference of up to 20°C between the individual thermal probes was recorded. The occurrence of the temperature stratification is related to the inlet gas velocity. This phenomenon was also observed in the HyTransfer project [4].

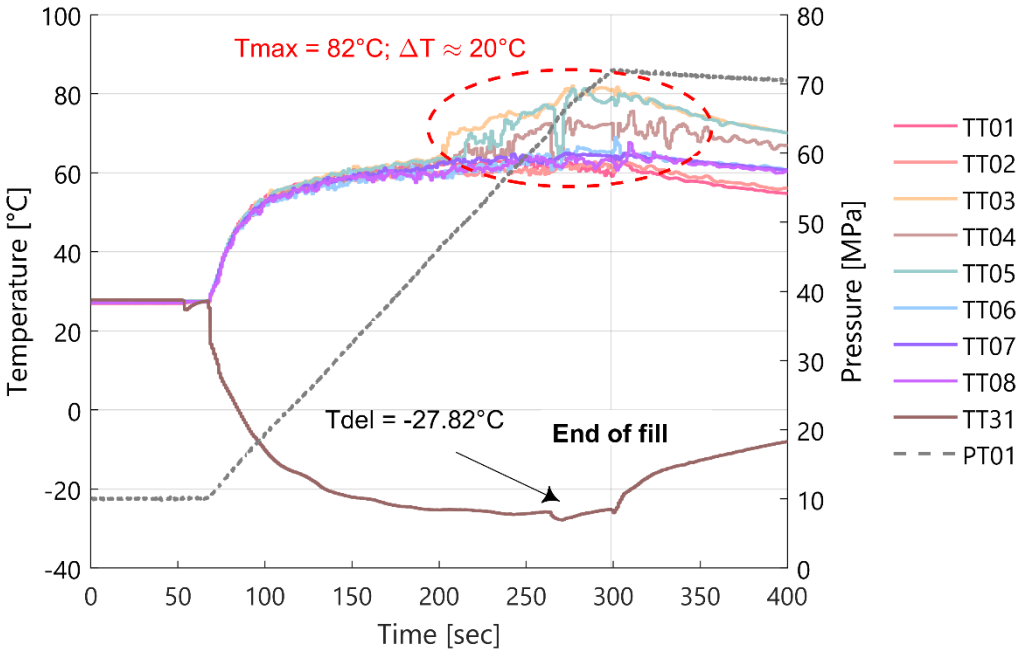

Figure 12 Fill n°2 (6 mm injection Ø) – pressure and temperature measurements during filling on the test bench with an APRR of 15.8 MPa/min (according to CEP protocol). For this experiment, the initial tank pressure was set to 10 MPa at an ambient temperature condition of 27.8°C

Based on calculations using the signal from the flow meter of the filling station, we were able to determine that the stratification occurred at a gas velocity of approx. 5 m/s. To ensure homogenous temperature conditions, an inlet gas velocity of over 5 m/s must be maintained throughout the entire filling process.

In order to increase the gas velocity at the intake, an alternative injection nozzle with a smaller diameter was tested. Figure 13 shows the measured pressure and temperature development of filling no. 3 using an injection nozzle with a diameter of 3 mm. For this experiment, the initial tank pressure was also set to 10 MPa at an ambient temperature of 21.5°C. Based on these initial conditions, the APRR was set to 19 MPa/min as per CEP A70 fueling protocol (ver. 2010).

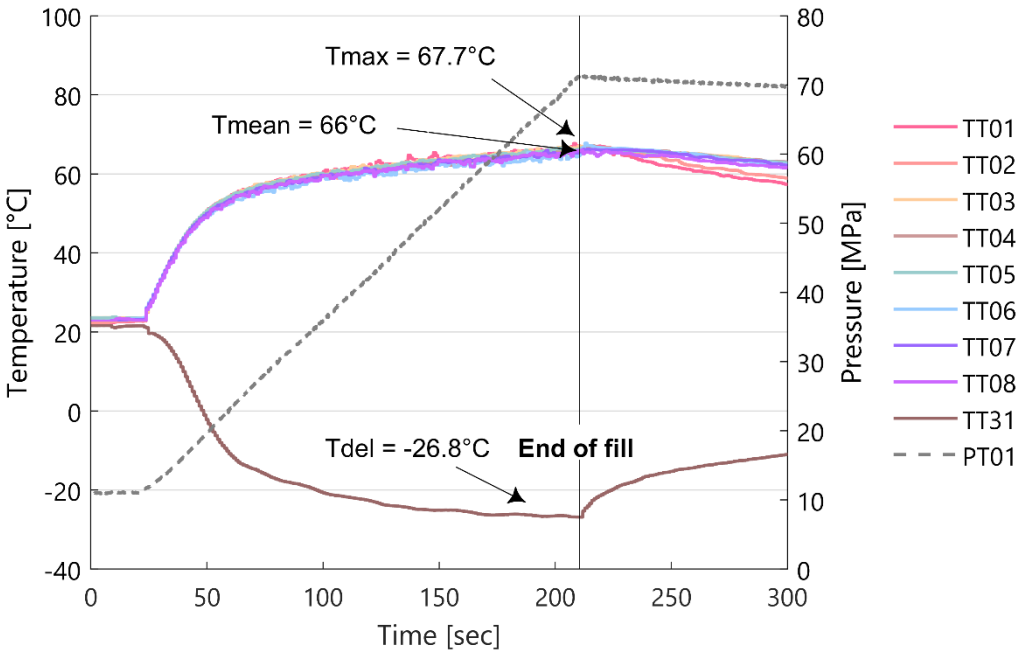

Figure 13 Fill n°3 (3 mm injection Ø) – pressure and temperature measurements during filling on the test bench with an APRR of 19 MPa/min (according to CEP protocol). For this experiment, the initial tank pressure was set to 10 MPa at an ambient temperature condition of 21.5°C

It can be seen that due to the increased injection velocities a homogenous temperature distribution was achieved throughout the whole fill. At the end of filling a difference of around 1.7°C was recorded between the mean and max temperature. Note that at first the temperature rises rapidly, but at some point the temperature rise in only marginal. This can be explained physically, since the temperature rise in the tank is mainly caused by the pressure rise. As soon as the hydrogen temperature inside the tank rises, the temperature difference between the hydrogen and the tank material creates a heat transfer from the gas region to the tank. The temperature development is dominated by these two competing physical phenomena. In addition, it can be seen that the temperature does not rise further when the target pressure is reached, as it is expected for a homogenous mixture. After filling is completed, the probes in the lower part of the tank (e.g. TT01 and TT02) measure a lower temperature, similar to the reference case.

Besides the switch to the CEP fueling protocol and the testing of an alternative injection nozzle filling no. 4 and 5 show the influence of different initial tank pressures. Figure 14 and Figure 15 show the measured pressure and temperature development of the two experiments. Both tests were carried out at similar ambient temperature conditions and therefore had a similar pressure ramp rate and achieved comparable precooling temperatures at the intake. Note that for filling no. 4 the initial tank pressure was lowered and set to 5 MPa, whereas in filling no. 5 the tank pressure was increased and initially set to 30 MPa. It can be seen that both tests showed a homogeneous temperature development similar to the filling no. 3. Furthermore, the higher the initial tank pressure, the lower the max temperature reached at constant APRR and same precooling conditions.

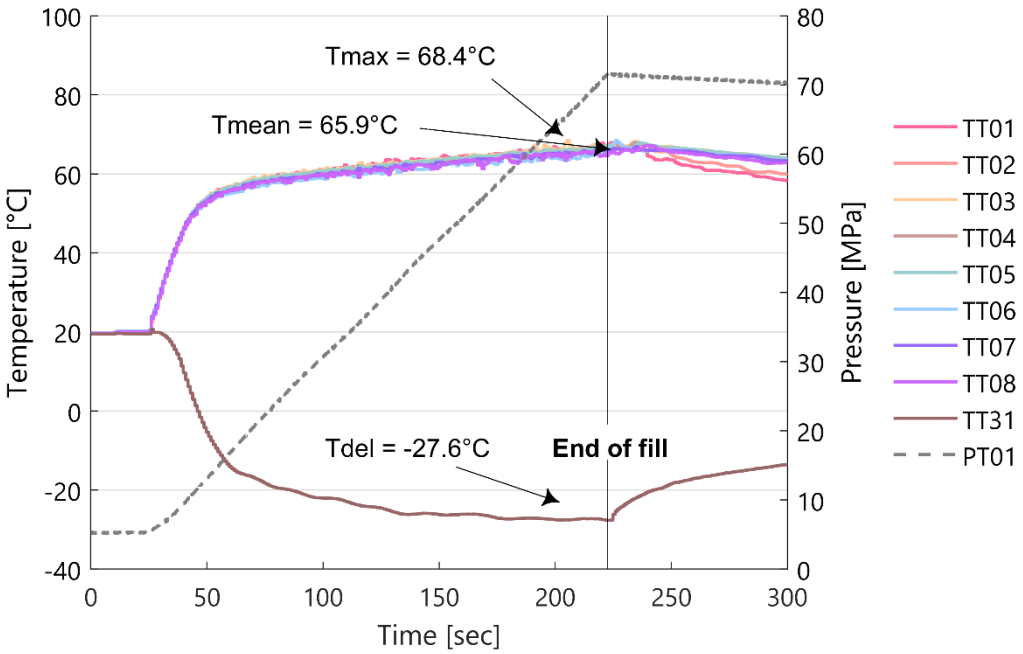

Figure 14 Fill n°4 (3 mm injection Ø) – pressure and temperature measurements during filling on the test bench with an APRR of 19.8 MPa/min (according to CEP protocol). For this experiment, the initial tank pressure was set to 5 MPa at an ambient temperature condition of 19.5°C

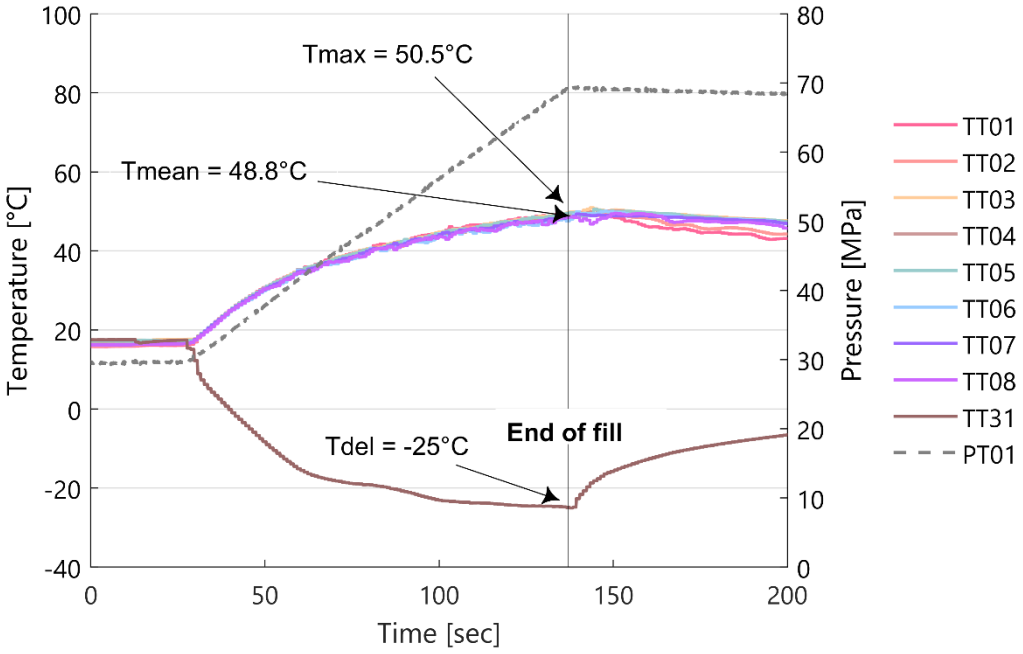

Figure 15 Fill n°5 (3 mm injection Ø) – pressure and temperature measurements during filling on the test bench with an APRR of 21.7 MPa/min (according to CEP protocol). For this experiment, the initial tank pressure was set to 30 MPa at an ambient temperature condition of 16°C

4.2 Simulation results

First, the simulation results of the reference case are compared with the measurements. Then a model evaluation is presented showing the capabilities of the developed model.

The initial and boundary conditions of the case discussed below were chosen to fit the reference case of the experiments previously shown. A detailed description of the model setup can be found in Section 3.2. Figure 16 shows an example of predicted temperature profiles compared to experimental data for one of the thermocouples in the upper part of the tank (TT5). This particular thermocouple is considered as representative for reasons of clarity. It can be seen that the calculated temperatures initially show a good agreement up to t~20s, thereafter the model leads to a slight overestimation of the temperatures. The final temperature difference between model and measurement was 8.3°C (t = 131 s). Nevertheless, the characteristics of the measured profile are recognizable, e.g. the abrupt temperature rise after completion of refueling.

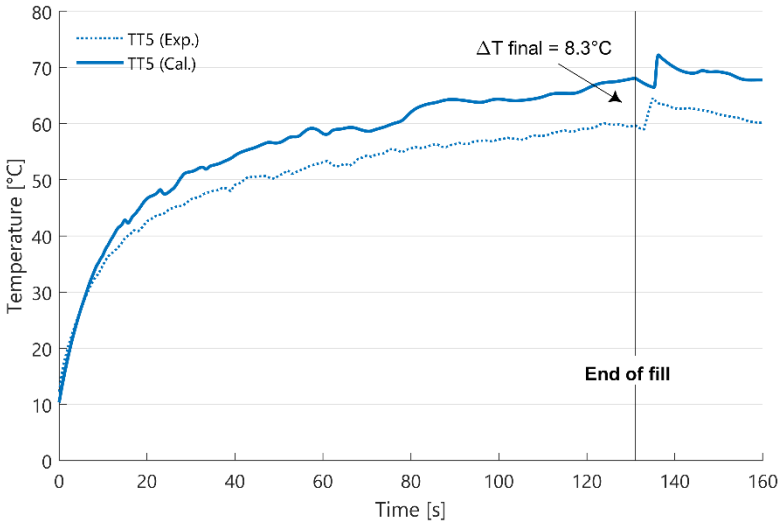

Figure 16 Temperature profile inside the tank: comparison of experimental data and simulation results of the reference case

Similar to our measurements, the simulation predicts an equivalent temperature rise after completion of filling. As already observed in our experiments, the reference case seems to be a borderline case for which the gas recirculation generated by the hydrogen jet is just good enough to prevent pronounced temperature stratification. Figure 17 shows in detail the temperature and velocity distribution in the vertical center plane at different times during the refueling process. The inlet is on the left side of the figures, as the low temperatures of the pre-cooled hydrogen reveal. Note that the tank is positioned horizontally and gravitational force is directed downwards.

At 25% of filling shown in 17 (a), the temperature field is nearly uniform with slightly lower temperature at the rear of the tank. The homogeneous temperature distribution can be explained by the high velocities at the inlet of approx. 16.5 m/s, which ensure good mixing of the cold incoming hydrogen with the compressed hydrogen inside the tank. Furthermore, it can be seen that a backflow occurs behind the injection pipe in the upper part of the cylinder.

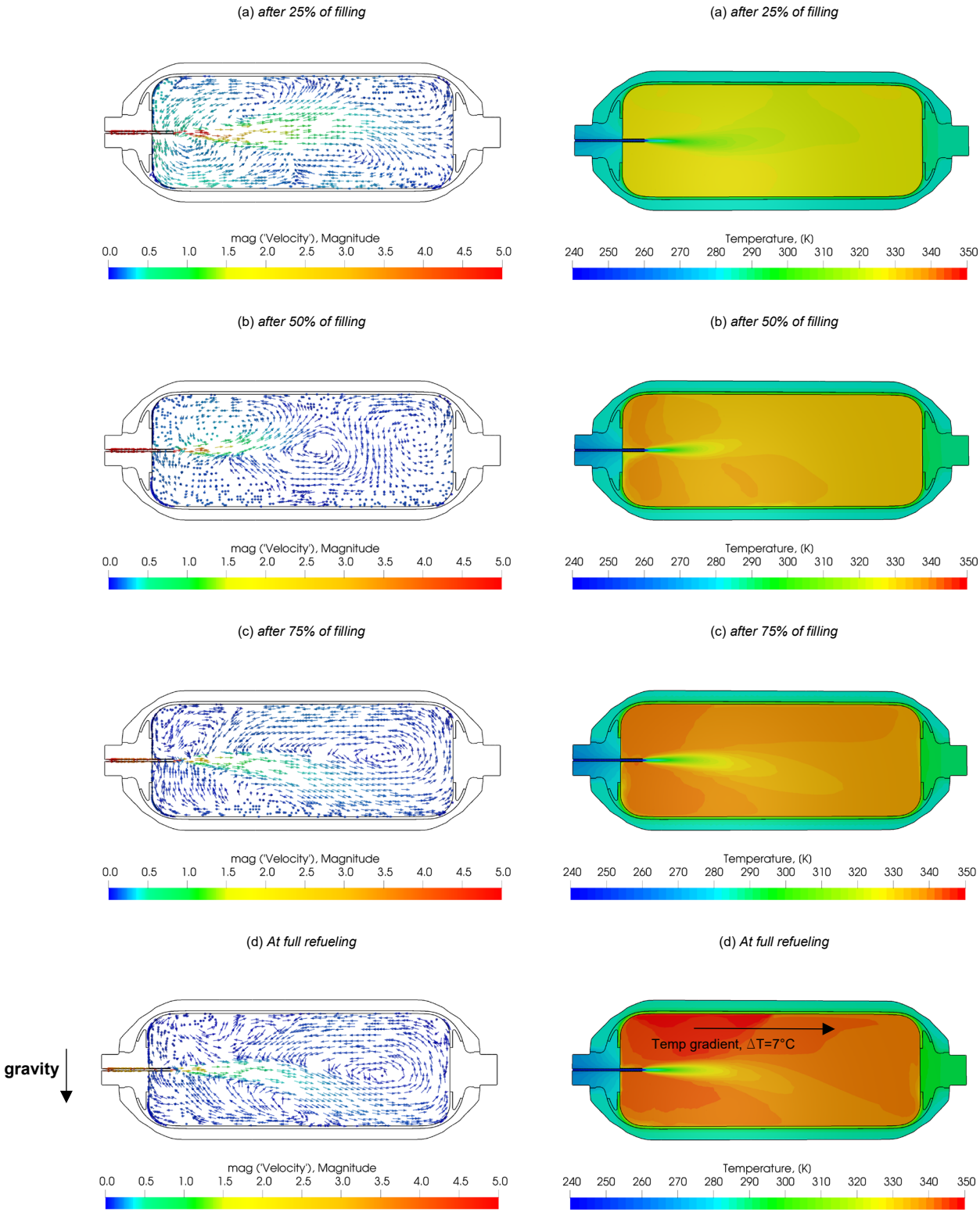

Figure 17 Temperature and velocity distribution in the test cylinder on the vertical cross section

After reaching half of the fueling and subsequently, as shown in 17 (b), (c), and (d), the velocity at the inlet decreases and the plume of the inflowing cold hydrogen is directed downwards. The hottest temperature zone is located in the upper left part of the tank, where the gas circulation first starts to sink and thus a temperature gradient develops. A temperature difference of up to 7°C can be observed. At reaching full refueling, as shown in 17 (d), the velocity at inlet was about 5 m/s. A further drop in velocity would lead to a vertical temperature stratification, as already observed experimentally.

In the following, we discuss the influence of the operating parameters on the final mass-averaged temperature achieved in the tank, as shown in Figure 18. It is shown that for higher pressure and temperature conditions imposed to the model, the final temperature also increases, while a decrease causes the opposite. In addition, it was shown that an increase in thermal conductivity of the liner material leads to a significant increase of the heat flux and therefore to a lower final temperature. It emerged that the liner conductivity influence the performance the most.

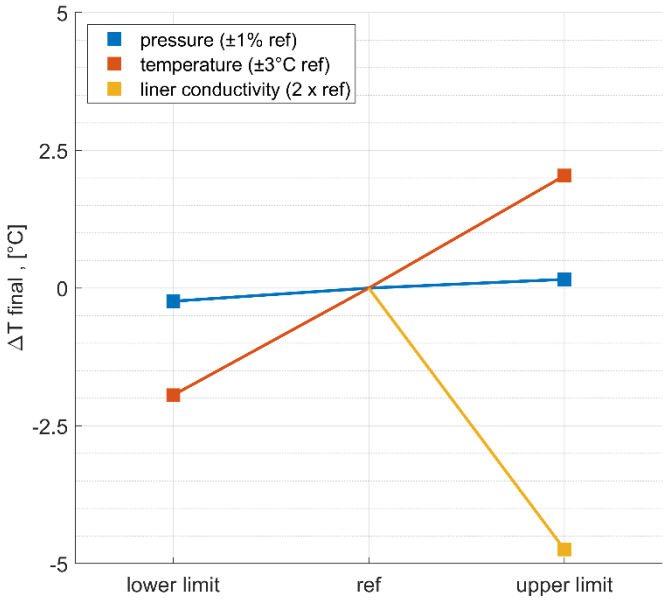

Figure 18 Influence of operating parameters and material properties on the final mass-averaged temperature inside the tank

With an increased liner conductivity, the calculated temperature profile shows good agreement with the experimental results. Figure 19 shows the predicted temperature profile of the TT5 thermocouple compared to the measurements of the reference case. In the case of the TT5 thermocouple, the difference of the calculated final temperature was 3.4°C (err. 5.5%). Note that the simulation showed a good overall agreement with the experimental data at all positions of the thermocouples, and errors on the calculated maximum fluid temperatures were below 6%.

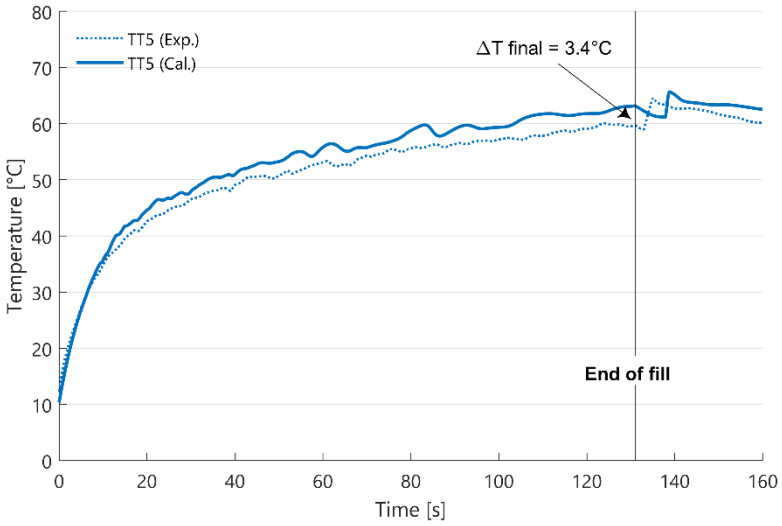

Figure 19 Temperature profile inside the tank: comparison of experimental data and simulation results of the reference case with increased thermal conductivity (2 x ref) of the plastic liner

In addition, it should be noted that not only the calculated temperature and pressure profile needs to match the experimental data, but also the mass delivered during refueling.

Figure 20 shows the mass-averaged temperature profile during refueling inside the tank for the equation of state of Peng-Robinson and Redlich-Kwong. Both equations of state reach a similar filling temperature, but in order to depict the difference of the results, the temperature curves are shown in relation to the state of charge. For a complete filling there is a difference of 6.25%, but note that a small difference is already visible at the beginning.

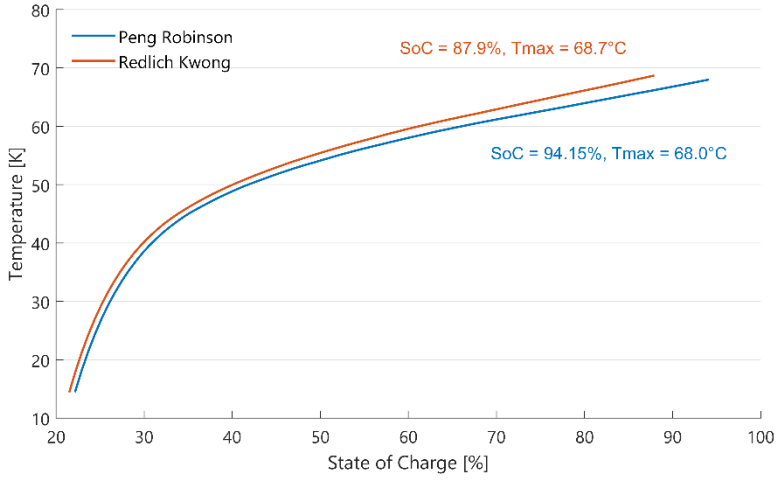

Figure 20 Temperature profile inside the tank: comparison between Peng-Robinson and Redlich-Kwong equation of state

The State of Charge (SOC) is the ratio of hydrogen density to the density at nominal working pressure rated at the standard temperature 15°C. SOC is expressed as a percentage and is computed based on the gas density per the formula below.

$$SOC\ (\%) = \frac{\rho(p,T)}{\rho(NWP, 15°C)} * 100$$

5 Discussion of results

The discussion of the results is divided into two parts. First, the experimental observations and findings are commented on, and then in a second part the lessons learned from the simulation are discussed.

The experiments with the 36 liters tank showed that depending on the inlet gas velocities a non-homogeneous temperature distribution can develop throughout the filling process. In filling no. 2, a temperature difference of up to 20°C between the individual thermal probes at a maximum temperature of 82°C was detected. However, it should be noted that all experiments were without communication between the test bench and the fueling system. In the event of a communication refueling, the target pressure lies 10% higher while the APRR remains constant. In such a case, the maximum allowed temperature of 85°C would have been exceeded under the same mixing conditions (same injection nozzle). Based on calculations using the signal from the flow meter of the filling station, the temperature stratification starts at an inlet gas velocity of less than 5 m/s. In filling no. 3, homogeneous temperature distribution was achieved with an alternative injection nozzle, which leads to higher velocities at the inlet. Note that it is important to have a temperature distribution that is as homogenous as possible during the entire filling process in order to have a good vehicle tank temperature control and therefore to ensure that the gas temperature stays within the specified limits of 85°C. The conventional system used in today's cars uses a single probe measurement. If the probe is placed in the cold part of the tank, it is possible that the temperature has already exceeded the 85°C but was not detected. Furthermore, the experiments showed that at higher initial tank pressure the maximum temperature reached was significantly lower. Such refueling do not require excessive hydrogen precooling and are subject to possible optimization. For such optimization, it is important that the infrared communication works reliable, as it is possible that the car owner has previously stopped a fueling and therefore already has an increased tank temperature.

The developed computational model was tested against the reference case measurement. The model overestimated the final reached temperature inside the tank with the parameter settings originally used. Nevertheless, the characteristics of the measured temperature profile were recognizable. The simulation predicted similar to the measurements an equivalent temperature rise after completion of filling. A detailed analysis of the temperature distribution, see Figure 17, showed that for the reference filling case the temperature gradient occurs for the first time in the upper left part of the tank. This seems to be plausible and corresponds to the findings of the experiments. Further sensitivity analysis on some of the main modelling parameters were carried out to assess the response of the model to variations in material properties and boundary conditions. It was shown that the predicted temperature inside the tank strongly depends on the material properties of the plastic liner. With an increased, but according to literature still plausible liner conductivity, the calculated temperature profile was found in good agreement with experimental data and errors on the calculated maximum gas temperatures were below 6%. Furthermore, it was shown that Peng-Robinson overestimates the density, while Redlich-Kwong's equation of state is more accurate, but underestimates the density at high pressure. Besides the density, it is crucial to accurately model all thermophysical properties of hydrogen, which is why we recommend the use of the standardized equation for hydrogen from NIST [9].

6 Conclusions and outlook

Finally, here we summarize the most important findings from the experimental and simulation activities.

The assessment of the pre-cooling system at Empa's HRS showed that under the current conditions a significant amount of energy is required. It was differentiated between the cooling energy required to pre-cool the dispensed hydrogen and the overhead cooling energy needed to keep the HX at a constant low temperature. The overhead consumption strongly depends on ambient conditions. On a warm summer day the electric energy required for the daily overhead cooling is in the order of 30 kWh_e. Whereas the electric energy needed for cooling the dispensed hydrogen is approximately 0.5 kWh_e/kg. Note that the energy intensity of a HRS highly depends on the utilization level of the station. As the HRS utilization level increases, the energy intensity gets smaller.

The experimental filling tests showed that the recirculation of the gas generated by the hydrogen jet at the inlet is important to achieve a homogeneous temperature distribution inside the tank. A vertical temperature stratification was observed when the inlet gas velocities fell below 5 m/s. As a consequence, temperature differences of up to 20°C between the individual thermos probes were detected. Homogeneous temperature distribution was achieved using a nozzle with an injection diameter of 3 mm, which leads to higher velocities at the inlet. Further it was shown that at higher initial tank pressure (>30 MPa) the maximum temperature (50.5°C) reached was significantly lower. Such refueling do not require excessive hydrogen precooling and are subject to possible optimization.

The developed computational model showed an accurate prediction of the temperature. Depending on model parameter settings, the calculated temperature profile was found in good agreement with experimental data and errors on the calculated maximum gas temperatures were below 6%. A sensitivity analysis showed that the predicted temperature strongly depends on the chosen conductivity of the liner material. Nevertheless, the CFD model proved to be a useful tool to get a better understanding of temperature stratification.

6.1 Next steps after end of project

With the CFD model developed, various additional aspects could be investigated to further deepen the understanding of the hydrogen filling process.

The sensitivity analysis should be extended to include studies on grid refinement in sensitive regions like the gas and tank wall interface. Further, the influence of the turbulence model on the results should be investigated in detail.

In addition, validation computations are necessary to take into account a wider range of conditions related to different ambient temperatures, different tank sizes and shapes, different tank types (e.g. tank type III) and different initial temperatures of hydrogen by pre-cooling. A validation of the CFD modeling strategy should also include the post-filling phases, e.g. holding time and tank emptying, to demonstrate the capabilities of the CFD model to describe all phases of tank use in a vehicle. It will then be a valuable tool, complementary to experimental campaigns to optimize refueling.

7 Publications

07/2019 *Conference Talk, Research in the field of gaseous hydrogen refueling to reduce the energy consumption of filling stations, European Fuel Cell Forum (EFCF)*

8 References

[1] *SAE J2601 Fueling Protocols for Light Duty Gaseous Hydrogen Surface Vehicles, SAE International, 2016*

[2] *Elgowainy A. et. al., Techno-economic and thermodynamic analysis of pre-cooling systems at gaseous hydrogen refueling stations, International Journal of Hydrogen Energy, 2017, vol. 42, pp 29067-29079*

[3] *ESI OpenCFD, OpenFOAM User Guide v1806 , openfoam.com, 2018, Version v1806*

[4] *HyTransfer Project, https://www.hytransfer.eu/, (online on the 13st of December 2019)*

[5] *Peng D. and Robinson D., A New Two-Constant Equation of State, Ind. Eng. Chem. Fund., 1976, vol. 15, no. 1, pp. 59-64*

[6] *Menter F., Two-equation eddy-viscosity turbulence models for engineering applications, AIAA Journal, 1994, vol. 32, no. 8, pp. 1598-1605*

[7] *Abhilash Suryan et al., Three dimensional numerical computations on the fast filling of a hydrogen tank under different conditions, International Journal of Hydrogen Energy, 37, 2012, 7600-7611*

[8] *O. Redlich and J.N.S Kwong, On the thermodynamics of solutions, Chem. Rev. vol. 44, pp. 233-244, 1949*

[9] *Eric W. Lemmon and Marcia L. Huber, Revised standardized equation for hydrogen gas densities for fuel consumption applications, Journal of Research of the National Institute of Standards and Technology, 2008*

9 Appendix

9.1 Appendix 1: Piping and instrumentation diagram of the test bench

Figure 21 shows the piping and instrumentation diagram (P&ID) of the realized test bench. The content in the blue box is mounted on the mobile frame. As illustrated in the diagram a nitrogen bottle can be connected to flush the pipes and tank before usage. After a filling procedure, the hydrogen stored in the tanks can be vented into the atmosphere through a blower connected to the tank.

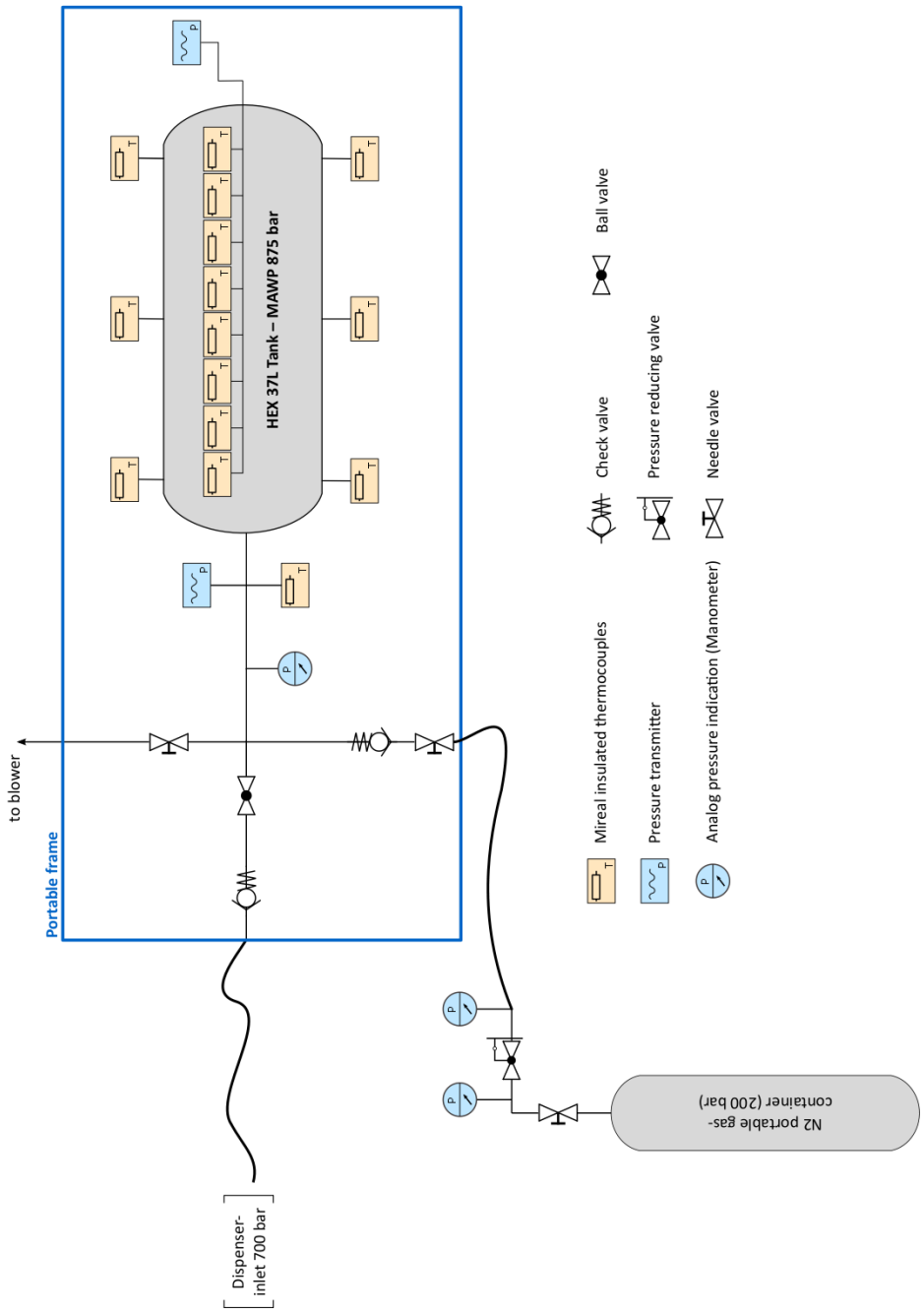

Figure 21 Piping and instrumentation diagram of the realized test bench